

# 1 Predictions of biodiversity are improved by 2 integrating trait-based competition with abiotic 3 filtering

4  
5 Loïc Chalmandrier<sup>1-3</sup>, Daniel B. Stouffer<sup>2</sup>, Adam S. T. Purcell<sup>4</sup>, William G. Lee<sup>5,6</sup>, Andrew J.  
6 Tanentzap<sup>7</sup>, Daniel C. Laughlin<sup>1</sup>

7  
8 1 Department of Botany, University of Wyoming, Laramie, Wyoming, USA

9 2 Centre for Integrative Ecology, School of Biological Sciences, Univ. of Canterbury, Christchurch, New Zealand

10 3 Theoretical Ecology, Faculty of Biology and Pre-Clinical Medicine, University of Regensburg, Regensburg,  
11 Germany

12 4 Tonkin + Taylor, Hamilton, New Zealand

13 5 Landcare Research, Private Bag 1930, Dunedin 9054, New Zealand

14  
15 6 School of Biological Sciences, University of Auckland, Private Bag 92019, Auckland 1142, New Zealand

16  
17 7 Ecosystems and Global Change Group, University of Cambridge, Cambridge, UK CB2 3EA

18

19  
20 All organisms must simultaneously tolerate the environment and access limiting resources if  
21 they are to persist. Otherwise they go extinct. Approaches to understanding environmental  
22 tolerance and resource competition have generally been developed independently. Consequently,  
23 integrating the factors that determine abiotic tolerance with those that affect competitive  
24 interactions to model species abundances and community structure remains an unresolved  
25 challenge. This is likely the reason why current models of community assembly do not  
26 accurately predict species abundances and dynamics. Here, we introduce a new synthetic  
27 framework that models both abiotic tolerance and biotic competition by using functional traits,  
28 which are phenotypic attributes that influence organism fitness. First, our framework estimates  
29 species carrying capacities that vary along abiotic gradients based on whether the phenotype  
30 tolerates the local environment. Second, it estimates pairwise competitive interactions as a  
31 function of multidimensional trait differences between species and determines which trait  
32 combinations produce the most competitive phenotypes. We demonstrate that our combined  
33 approach more than doubles the explained variance of species covers in a wetland community  
34 compared to the model of abiotic tolerances alone. Trait-based integration of competitive

1

35 interactions and abiotic filtering improves our ability to predict species abundances across space,  
36 bringing us closer to more accurate predictions of biodiversity structure in a changing world.

## 37 **Introduction**

38 Predicting species abundances is a major focus of community ecology (McGill et al. 2006). In  
39 recent decades, trait-based ecology has proposed that species morphological, physiological or  
40 phenological features determine how abiotic filtering and species interactions affect local  
41 community structure (Violle et al. 2007; Kraft et al. 2015b). However, trait-based analyses of  
42 communities often focus on functional diversity (Spasojevic et al. 2014; Chalmandrier et al.  
43 2017) and few explicitly model species abundances (Zakharova et al. 2019).

44 Trait-based models of abiotic filtering that predict species abundances (Shipley 2010; Laughlin  
45 et al. 2012) assume that there are optimum trait values within a given environment, and species  
46 able to attain these trait values will be more likely occur in that environment (Kraft et al. 2015b).  
47 The most significant limitation of these models is that they fail to incorporate biotic interactions.  
48 In contrast, theoretical models of species interactions have a long and storied history in ecology  
49 (Lotka-Volterra 1925; Chesson 2000), and have been used to understand the foundational  
50 conditions for coexistence among competing species. For species to coexist stably, niche  
51 differences among species must be greater than differences in competitive ability (Chesson  
52 2000; Adler et al. 2007) and recent work suggests that those differences can be linked to  
53 functional traits (Kraft et al. 2015a).

54 Three primary obstacles have prevented the mathematical integration of models of abiotic  
55 filtering and models of species interactions. First, they lack a common numerical currency  
56 through which they could be linked. Trait-based models of abiotic filtering yield probabilities  
57 that a species occurs in an environment given its traits, whereas models of species interactions  
58 describe dynamics of populations over time given growth rates, carrying capacities, and  
59 pairwise interaction coefficients (Lotka-Volterra 1925; Chesson 2000). Second, the complexity  
60 of estimating pairwise interactions increases exponentially with the number of species in the  
61 community, and there has been no obvious method for estimating interaction coefficients  
62 without implementing laborious competition experiments (Kraft et al. 2015a). Finally, there  
63 have been no adequate tools to model classical community ecology sampling schemes. For  
64 instance, plant abundance is often visually assessed through percent cover classes that do not  
65 necessarily fit well with existing statistical frameworks. Recently, authors have formalized the

66 use of beta distributions to adequately model these sampling schemes (Damgaard & Irvine  
67 2019), but they have yet to be implemented in biodiversity modeling.

68 Here we present a new synthetic framework that overcomes these three obstacles. This  
69 framework, which we call Banquo, integrates TraitSpace, a trait-based model of abiotic filtering  
70 (Laughlin et al. 2012), with a Lotka-Volterra competition model. First, we assume that the  
71 probability that a species occurs in an environment given its traits is proportional to its local  
72 carrying capacity, *i.e.*, the maximum population size that a species can reach given local  
73 resources and abiotic conditions in the absence of competition (MacArthur & Levins 1967).  
74 Second, we assume pairwise interaction coefficients are a function of observed trait differences  
75 between species, thereby substantially reducing the number of parameters needed to estimate  
76 pairwise interaction coefficients (Chalmandrier et al. 2021). Drawing inspiration from  
77 coexistence theory (Chesson 2000; Adler et al. 2007), the parameterization of this function  
78 allows for competitive outcomes to be affected to differing degrees by both niche partitioning  
79 (*i.e.*, strong competitive interference among functionally similar species) and competitive  
80 hierarchies (*i.e.*, species have strong competitive impacts on species with inferior trait values).  
81 Third, we use the recent methodological developments of Irvine et al. (2019) to link the output  
82 of our framework to observed plant species abundances that were estimated through cover  
83 classes.

84 We illustrate our framework by modeling plant species abundances along a flooding gradient in  
85 an ephemeral wetland (Purcell et al. 2019). After presenting our framework, we calibrated  
86 sixteen assembly models that include abiotic filtering and/or biotic filtering tested on different  
87 sets of functional traits. Then, we compared the statistical performance of these sixteen  
88 assembly models. Finally, we analyzed how the parameterization and output of the calibrated  
89 models inform our knowledge about the assembly of wetland plant communities.

## 90 Methods

### 91 The framework

#### 92 *Step 1 – Estimating species carrying capacities along environmental gradients*

93 We started with the Traitspace framework to model species' probabilities of occurrence along  
94 the flooding gradient (Laughlin et al. 2012). Traitspace characterizes the size and shape of the  
95 environmental filter based on a multivariate linear model with a vector of individual plant traits  
96 ( $T$ ) as the response and a vector of environmental gradients ( $E$ ) as the predictors, i.e. the  
97 function  $T = f(E_k)$ . Traitspace uses this linear model to estimate the conditional distributions of  
98 traits  $T$  given the environmental conditions in site  $k$  ( $P(T|E_k)$ ). Second, it uses the intraspecific  
99 trait distribution of each species across sites, i.e. the conditional distributions of traits given  
100 species identity ( $P(T|S_i)$ ). The posterior distribution of species presence  $S_{ik}$  of species  $i$  in site  $k$   
101 is conditioned on both the trait state  $T$  and the environmental conditions  $E_k$ .  $P(S_{ik}|T, E_k)$  is  
102 computed using Bayes theorem:

103

$$104 \quad P(S_{ik}|T, E_k) = \frac{P(T|S_i)P(S_{ik})}{\sum_i P(T|S_i)P(S_{ik})} \quad (1)$$

105 The desired posterior is computed by integrating with respect to traits to obtain the probability  
106 of occurrence of a species given the environmental conditions:

$$107 \quad P(S_{ik}|E) = \int P(S_{ik}|T, E_k)P(T|E_k)dT \quad (2)$$

108 In practice, we use Monte Carlo integration to estimate the average probability of presence of  
109 each species in each site by randomly sampling 500 trait values per site based on the estimated  
110 trait-environment relationship ( $T = f(E)$ ) and then averaging the probability distribution for each  
111 site and each species. In the end, we obtained a site-by-species probability table.

112 We then assumed that the carrying capacity (in percent cover)  $K_{ik}$  of species  $i$  in a site  $k$  can be  
113 estimated from its probability of presence in that site using an increasing log-log function:

$$114 \quad K_{ik} = a \left( \frac{P(S_{ik}|E_k)}{\max_{i,k}(P(S_{ik}|E_k))} \right)^b \quad (3)$$

115 with  $a \in [0, 1]$ ,  $b \in \mathbb{R}^+$ .

116 We standardized the probability value  $P(S_{ij}|E_j)$  by the maximum value across all species  $i$  and all  
117 sites  $j$  to ensure that carrying capacities  $K_{ij}$  are all set between 0 and 1 (as a percent cover  
118 variable).

119 **Step 2 – Modeling the biotic filter: estimation of trait-mediated plant competitive interactions**

120 **Formulation of the interaction matrix** – Here we assume that the interaction coefficient  $\alpha_{ik}$   
121 that measures the competitive impact of species  $j$  on species  $i$  can be estimated as a function of  
122 difference in traits. We test a formulation of  $\alpha_{ij}$  as a function of the empirical trait of value  $t_i$  of  
123 species  $i$  and  $t_j$  of species  $j$ :

$$124 \quad \alpha_{ij} = \begin{cases} C \times \frac{1}{\sigma\sqrt{2\pi}} \exp\left[-\frac{1}{2}\left(\frac{t_j - t_i - \mu}{\sigma}\right)^2\right] & \text{if } i \neq j \\ 1 & \text{if } i = j \end{cases} \quad (4)$$

125 with  $C \in \mathbb{R}^+$ ,  $\mu \in \mathbb{R}$ ,  $\sigma \in \mathbb{R}^+$ .

126 Interspecific coefficients followed a modified Gaussian function of trait differences where  $\mu$  is  
127 the peak position of the Gaussian,  $\sigma$  is its width, and  $C$  controls the amplitude of interspecific  
128 coefficients relative to intraspecific coefficients. Species intraspecific coefficients were fixed to

129 1. For a small values of the ratio  $\frac{C}{\sigma\sqrt{2\pi}}$ , the matrix of interaction coefficients can be

130 approximated by the identity matrix ( $\alpha = \mathbf{I}$ ) and estimated species covers simplify to the vector  
131 of carrying capacities. For large values of  $\sigma$  ( $\sigma \rightarrow \infty$ ), interspecific coefficients are all equal to

132  $C' = \frac{C}{\sigma\sqrt{2\pi}}$  and represent a situation where interspecific interactions among species are

133 constant and do not depend on species traits.

134 The formulation of equation 4 is that it can be directly related to either competitive hierarchies  
135 or niche partitioning (Chesson 2000; Adler et al. 2007). The value of the parameter  $\mu$  defines if  
136 the studied trait relates more to niche partitioning among species, hierarchical competition, or a  
137 mixture of the two. Specifically, for  $\mu$  close to 0, pairwise interaction coefficients are high for  
138 small trait differences and low for large trait differences, indicating a predominance of niche  
139 partitioning among species (Supplementary figure 1-A). For a low value of  $\mu$ , the left hand part  
140 of the bell-shaped curve falls outside of the range of observed trait differences. Thus the curve  
141 approaches a monotonically decreasing function that indicates a predominance of competitive  
142 hierarchy: species with a large trait value are competitively superior over species with small trait  
143 values (Supplementary figure 1-B). Conversely, a high value of  $\mu$  returns a monotonically  
144 increasing function that indicates a predominance of hierarchical competition with species with

145 a small trait value being competitively superior over species with large trait values. Intermediate  
 146 situations (moderately large or moderately small values of  $\mu$ ) indicate a mixture of niche  
 147 partitioning and hierarchical competition (Supplementary figure 1-C): niche partitioning is  
 148 predominant among species with large trait differences, but among species with small trait  
 149 differences, competition is not symmetric (as in a case of “pure” niche partitioning”) and  
 150 hierarchical competition is the predominant coexistence process.

151 Finally, our formulation of interaction coefficients can be extended to multiple trait dimensions  
 152 using a modified multivariate Gaussian function. In this study, we used a maximum of two trait  
 153 dimensions in which case interaction coefficients were formulated as follows:

154

$$155 \alpha_{ij} = \begin{cases} \frac{C}{2\pi\sigma_1\sigma_2\sqrt{1-\rho^2}} \exp\left[-\frac{1}{2(1-\rho^2)}\left[\left(\frac{t_{1,j}-t_{1,i}-\mu_1}{\sigma_1}\right)^2 + \left(\frac{t_{2,j}-t_{2,i}-\mu_2}{\sigma_2}\right)^2 - 2\rho\frac{(t_{1,j}-t_{1,i}-\mu_1)(t_{2,j}-t_{2,i}-\mu_2)}{\sigma_1\sigma_2}\right]\right] & \text{if } i \neq j \\ 1 & \text{if } i = j \end{cases}$$

156 with  $C \in \mathbb{R}^+$ ,  $\mu \in \mathbb{R}$ ,  $\sigma_1 \in \mathbb{R}^+$ ,  $\sigma_2 \in \mathbb{R}^+$ ,  $|\rho| < 1$ . (5)

157 This equation describes a two-dimensional symmetric Gaussian function of trait differences of  
 158 peak position ( $\mu_1$ ,  $\mu_2$ ) and of widths  $\sigma_1$  and  $\sigma_2$  across the first and second dimensions. Properties  
 159 and interpretations of the parameters are similar to their uni-dimensional counterparts. The two-  
 160 trait formulation includes an additional coefficient  $\rho$  between the two trait difference dimensions  
 161 that determine if trait differences independently contribute to the pairwise interaction  
 162 coefficients ( $\rho = 0$ ) or if they interact ( $0 < |\rho| < 1$ ).

### 163 **Step 3 - Integrating the abiotic and biotic filter with Lotka-Volterra models**

164 We assumed that species’ dynamics could be modeled through a Lotka-Volterra competition  
 165 model:

$$166 \frac{1}{N_{ik}} \frac{dN_{ik}}{dt} = \frac{r_{ik}}{K_{ik}} (K_{ik} - \sum \alpha_{ij} N_{jk}) \quad (6)$$

167 where  $N_{ik}$  and  $r_{ik}$  are, respectively, the percent cover and the intrinsic growth rate of species  $i$  in  
 168 site  $k$ .

169 Within this model, the vector of all strictly positive species covers at equilibrium  $N_k^*$  satisfies  
 170 the equation:

$$171 N_k^* = \alpha^{-1} K_k$$

172 where  $\mathbf{K}_k = \{K_{ik}\}$  is the vector of species carrying capacities, and  $\alpha = \{\alpha_{ij}\}$  is the matrix of per-  
173 capita effects estimated as described above.

174 For a given set of parameters, the interaction matrix  $\alpha$  was estimated, the Moore-Penrose inverse  
175 of  $\alpha$  was computed, and multiplied to each site's vector of species carrying capacities estimated  
176 from the TraitSpace model. Species local cover estimated in this way can be negative, reflecting  
177 that this equilibrium state is not feasible. To find a feasible equilibrium, for each vector of  
178 equilibrium species covers, we sequentially set to 0 the species with the most negative cover and  
179 re-estimated the equilibrium state. This procedure was repeated until finding an equilibrium  
180 state where all remaining species covers were positive.

### 181 **A test of the framework**

182 We tested our framework on a dataset of an ephemeral wetland in New Zealand (latitude  
183 44.374143°S, longitude 169.890052°E). In that ecosystem, plant community structure vary  
184 along a continuous flooding gradient. In this test, we assumed that plant community assembly is  
185 determined by the filtering of three functional traits by flooding duration that filters three  
186 functional traits (root porosity, height and SLA) and above-ground competition determined by  
187 height and SLA.

188 Analyses of the dataset are available in previous studies (Tanentzap et al. 2014; Tanentzap &  
189 Lee 2017; Purcell et al. 2019). Detailed methods about data collection are available in the  
190 supplementary materials. We analyzed the vegetation structure with a subset of the complete  
191 dataset (see Supplementary materials): 67 quadrats 25 × 25 cm in size set along four transects  
192 that run from the lowest point of the basin and advancing upslope to the kettlehole margin.  
193 Foliar cover was estimated for each species using the following cover estimates: 0.5%, 1%, 2%,  
194 3%, 4%, 5%, 10%, 15%, 20%, 30%, 40%, ..., 100%. We restricted the analysis to the 15 most  
195 abundant species in the study area for which we sampled traits on at least 20 individuals. These  
196 species collectively represent at least 80% of the total of plant cover in each quadrat (Pakeman  
197 & Quested 2007).

198 Root porosity, as a percentage variable, was logit-transformed. Height and SLA trait values were  
199 log-transformed prior to the analysis to approach a normal distribution. We modeled the  
200 relationship between root porosity, SLA, height and the flooding gradient and weighted trait  
201 observations by species cover.

202 The intraspecific trait distribution of each species was modeled using a multivariate normal  
203 distribution (R-function *mclust::dens Scrucca et al. 2016*). We then modeled the probability of  
204 occurrence of each species in each site given the local duration of flooding using the Traitspace  
205 framework described earlier.

206 To calibrate the interaction matrices, we used species maximum height along the gradient  
207 (calculated as the 95% quantile of each species height values) and species average SLA.  
208 Maximum height and SLA were moderately correlated ( $r = -0.42$ ,  $t = -1.65$ ,  $df = 13$ ,  $p = 0.12$ ).  
209 To avoid using correlated functional traits to estimate the two-traits interaction matrices, we first  
210 computed a PCA on the species by trait matrix containing species maximum height and average  
211 SLA. We then used species scores along these two PCA trait axes to calibrate the pairwise  
212 interaction matrix. As we used all the PCA dimensions, this step does not compromise the  
213 amount of trait variation used to estimate the two-trait interaction matrix. Practice showed us  
214 that, compared to using correlated (but tangible) functional traits, this extra step facilitates and  
215 speeds the convergence of the model calibration algorithm described below. However, we  
216 related pairwise interaction coefficients to the observed species functional traits values, rather  
217 than to the PCA trait axes, to facilitate the ecological interpretation of our results.

218 Using the Banquo framework, we tested a total of sixteen assembly models. All sixteen  
219 assembly models aim to solve the following equation to estimate the matrix of species cover  $N^*$   
220 at equilibrium:

$$221 \quad a \left( \frac{P(S_{ik}|E_k)}{\max_{i,k}(P(S_{ik}|E_k))} \right)^b - \alpha N_k^* = 0 \quad (7)$$

222 (Model 1) One null model without any assembly processes: species probability of presence  
223 given local abiotic conditions were assumed to be equally abundant in every site ( $b = 0$ ) and  
224 there is no interspecific competition (the interaction matrix  $\alpha$  is equal to the identity matrix  $\mathbf{I}$ ).

225 (Model 2) One abiotic filtering model: species probability of presence are estimated by the  
226 Traitspace framework ( $b > 0$ ) and there is no interspecific competition ( $\alpha = \mathbf{I}$ ).

227 (Models 3-7) Five biotic filtering models that include no abiotic filtering: species probability of  
228 presence were assumed to be equal across species and in every site ( $b = 0$ ) but species cover is  
229 determined by interspecific competitive interactions ( $\alpha \neq \mathbf{I}$ ) that could depend on 3) no traits  
230 ( $\sigma \rightarrow \infty$ ), 4) plant height, 5) SLA, 6) both height and SLA without the interaction parameter  $\rho$ , or  
231 7) both height and SLA with the interaction parameter  $\rho$ .



232 (Models 8-12) Five abiotic and biotic filtering models: species probability of presence are  
233 estimated by the Traitspace framework ( $b > 0$ ) and species cover is also impacted by  
234 interspecific competitive interactions ( $\alpha \neq \mathbf{I}$ ) that could depend on 8) no traits ( $\sigma \rightarrow \infty$ ), 9) plant  
235 height, 10) SLA, 11) both height and SLA without the interaction parameter  $\rho$ , or 12) both  
236 height and SLA with the interaction parameter  $\rho$ .

237 We summarize the characteristics of each assembly model and their parameters in Table 1.

### 238 ***Calibration and comparison***

239 We used the likelihood function proposed by Irvine et al. (2019) given that observed species  
240 covers were recorded as percent cover classes. Briefly, the likelihood function links the ordinal  
241 observations of plant cover to a latent beta distribution of mean  $N_{ij}$  (in our case estimated by the  
242 assembly models) and uncertainty parameter  $\phi$ , that can be interpreted as a measure of plant  
243 spatial aggregation (Damgaard & Irvine 2019). One drawback of using the beta distribution is  
244 that it cannot model zero percent covers. To circumvent that issue, we added a small offset (0.05  
245 %) to zero percent cover values, as suggested by Irvine et al. (2019). Note that this corresponds  
246 to moving unobserved species up to the next highest cover class, that only included a single  
247 cover values (0.1% of the total number of cover values).

248 Depending on the assembly models, there were two (null model) to nine parameters (abiotic +  
249 biotic model with height and SLA with the interaction parameter  $\rho$ ) to estimate. We set  
250 regularizing priors on all parameters (Banner et al. 2020): we avoid making *a priori* assumptions  
251 about the nature of the relationship between traits, carrying capacities, pairwise interactions and  
252 species cover but we limited the extent of the parameter space that was uninformative. Details  
253 about the prior functions and their hyper-parameterization are available in the supplementary  
254 materials.

255 We used a Differential-Evolution Markov-Chain Monte Carlo algorithm (DEzs MCMC in the R-  
256 package BayesianTools (Hartig et al. 2017) to estimate the posterior distributions of the  
257 parameters. For each model, we ran four chains for  $6 \times 10^5$  steps. Convergence was assessed  
258 through Gelman's multivariate convergence criterion (MPSRF, Gelman et al. 2014).

259 ***Assembly model comparison*** – We compared the fits of the calibrated models using two metrics:  
260 the Deviance Information Criterion (DIC, Gelman et al. 2014) and Nagelkerke's pseudo  $R^2$   
261 metric (Nagelkerke 1991) which lends itself well to models that use a beta distribution and gives  
262 an indication of the variance they explain (Nakagawa & Schielzeth 2013). Nagelkerke's pseudo

263  $R^2$  was calculated from the ratio of a model's posterior likelihood and the likelihood of the null  
264 model (see above). Furthermore, we evaluate the ability of the models to predict species  
265 presence/absence by evaluating receiver operating characteristic curve (ROC) and the area under  
266 the curve (AUC) scores of each assembly model of the predicted species-site matrix using the R-  
267 package pROC (Robin et al. 2011).

268 **Code availability.** The R-scripts and data to run the analysis are available at  
269 <https://github.com/LoicChr/Banquo>

## 270 Results

### 271 Relationship between flooding and functional traits

272 Root porosity increased significantly with flooding duration ( $t = 7.714$ ,  $df = 224$ ,  $P < 0.0001$ .  
273 Adjusted  $R^2 = 0.206$ , Figure 1). Plant height decreased ( $t = -3.91$ ;  $df = 224$ ,  $P = 0.0001$ ) and  
274 specific leaf area increased with flooding duration ( $t = -3.10$ ;  $df = 224$ ,  $P = 0.002$ ) but these  
275 relationships explained only a negligible portion of trait variation along the flooding duration  
276 gradient (Height adjusted  $R^2$ : 0.036; SLA adjusted  $R^2$ : 0.060).

### 277 Model comparison

278 All assembly models but one converged (Gelman's multivariate convergence criterion inferior to  
279 1.1). Regardless of the performance statistic, there was a clear hierarchy across the assembly  
280 models (Table 1). The biotic models without abiotic filtering performed the worst (DIC:  
281 [2415.2, 2491.8], median pseudo  $R^2$ : [0.001, 0.088], AUC: [0.44, 0.68]). The biotic model  
282 calibrated with both height and SLA (with interaction term) had a convergence criterion of 1.81;  
283 we thus could not calculate its DIC and AUC. The associated pseudo  $R^2$  was however low  
284 across its posterior distribution: [0.056, 0.088]. The abiotic model without biotic interactions  
285 performed better (DIC: 2413, median pseudo  $R^2$ : [0.075, 0.085], AUC: 0.67).

286 The models that included both abiotic filtering and biotic interactions performed the best both in  
287 explained plant cover variance (pseudo  $R^2$ : [0.082, 0.196]; DIC: [2291.0, 2412.0]) and species  
288 presence/absence (AUC: [0.67, 0.77]). The model that assumed fixed pairwise interaction  
289 coefficients among competitive species was the worst performing of all (pseudo  $R^2$ : 0.081; DIC:  
290 2412.0, AUC = 0.67), while the SLA-based interaction models were the best performing.  
291 Among the latter, the model that calibrated biotic interactions using specific leaf area was the  
292 best fitting (DIC: 2291.0, pseudo  $R^2$ : 0.196, AUC: 0.77).

## 293 **Calibrated pairwise interaction matrices**

294 Among the assembly models that included both abiotic filtering and a pairwise interaction  
295 matrix calibrated with functional traits, the pairwise interaction matrix calibrated with SLA was  
296 the best supported by the data. It indicated a predominance of niche partitioning. There was a  
297 slight but non-significant hierarchical competition effect ( $\mu$ : 95% IQ [-0.43, 0.08], Figure 2C).  
298 This showed that the modest hierarchical competition among pairs of species conferred an  
299 advantage to species with the largest SLA.

300 All three pairwise interaction matrices calibrated with SLA were similar regardless of the  
301 inclusion of height or the interaction parameter  $\rho$ . At the median of their respective posterior  
302 distribution, the pairwise interspecific competition coefficients were strongly correlated ( $r =$   
303 0.82 between the SLA-calibrated matrix and the Height + SLA calibrated matrix without  
304 interaction;  $r = 0.98$  between the SLA-calibrated matrix and the Height + SLA calibrated matrix  
305 with interaction).

## 306 **Comparison between the abiotic model and the abiotic and biotic** 307 **assembly models**

308 We compared the abiotic model to the best assembly model (i.e. abiotic and biotic with pairwise  
309 interactions calibrated with Height and SLA without interaction). The abiotic model tends not to  
310 predict species absences well. The distribution of cover values was thus approximately normal  
311 around a median value of 3.30% (Supplementary Figure 5). Consequently, species presence  
312 along the flooding gradient was often overestimated with numerous species being predicted to  
313 be present in sites where they were not observed (e.g. see *Epilobium angustum*, Figure 3). In  
314 contrast, when biotic interactions are included, the assembly model tends to predict more  
315 absences and less even percent cover values among species (Figure 3, Supplementary Figure 5).

## 316 **Discussion**

317 Predictive models of community assembly have focused on incorporating abiotic filters and  
318 have generally ignored biotic interactions. Here we show that trait-based assembly rules can be  
319 used to directly model species abundances in communities by simultaneously accounting for  
320 both abiotic filtering and competitive interactions (Keddy 1992, 2001). There are two major  
321 implications of this study. First, we introduced a trait-based formulation of pairwise competitive  
322 interactions that allowed us to calibrate 210 interaction coefficients from observational data with  
323 no more than eight parameters. This new approach substantially improves our ability to infer  
324 interaction matrices with little additional complexity (Cabral et al. 2017; Chalmandrier et al.

325 2021). Second, the inclusion of competitive interactions among species improved predictions of  
326 local plant cover, which bolsters the argument that the modeling of species distribution must  
327 include both abiotic tolerances and species interactions (Alexander et al. 2015; Evans et al.  
328 2016).

329 The core feature of the Banquo model is the formulation and calibration of pairwise competition  
330 coefficients among species. We proposed a new flexible formulation of competitive pairwise  
331 interactions as a function of trait differences. Compared to estimating pairwise interaction  
332 coefficients individually, this considerably reduces the number of parameters to estimate  
333 (Zakharova et al. 2019; Chalmandrier et al. 2021). That formulation was directly inspired by,  
334 and thus constrained by, the principles of coexistence theory and how it has informed the study  
335 of functional diversity patterns (Chesson 2000; HilleRisLambers et al. 2012).

336 Traditionally, functional diversity pattern studies have assumed that niche partitioning was the  
337 main competition mechanism behind community assembly (MacArthur & Levins 1967). In that  
338 framework, niche partitioning would promote the coexistence of functionally dissimilar species  
339 and oppose itself to environmental filtering that promotes the coexistence of functionally similar  
340 species. In recent years, this framework has been criticized (Kraft et al. 2015b; Münkemüller et  
341 al. 2020) as coexistence theory posits that competition can also promote the coexistence of  
342 functionally similar species through hierarchical competition. Our framework has the benefit of  
343 not assuming niche partitioning or hierarchical competition as the main trait-based competitive  
344 mechanism among species, but rather permits the fit of a mixture of the two processes. Our  
345 empirical example illustrates that the pairwise interaction matrices of the assembly models were  
346 consistent with strong niche partitioning among species but with a small yet significant degree  
347 of hierarchical competition among species with small trait differences. Our modeling of pairwise  
348 interactions aims to provide a general and flexible relationship between competition strength  
349 among plants and trait differences rooted in coexistence theory. However, it is essentially  
350 phenomenological and does not explicitly model the mechanisms behind plant-plant  
351 competition. Future developments may aim at formulating competition as an explicit function of  
352 species' ability to consume local soil resources Letten et al. (2017) or intercept light (Falster et  
353 al. 2017). Beyond competition, a more complex modeling of plant biotic interactions could  
354 include facilitative interactions or acknowledge that the nature of species interactions can shift  
355 along environmental gradients (Maestre et al. 2009; Bimler et al. 2018).

356 Our trait-based modeling approach explicitly specifies classical assembly mechanisms  
357 (HilleRisLambers et al. 2012) and evaluates their ability to predict species local abundance  
358 using common modeling statistics. Our case study showed that including both abiotic filtering  
359 and biotic interactions led to a net improvement of the modeling of species local abundances and  
360 of community structure. One of the limitations of established trait-based models is that they tend  
361 to overestimate species occurrences (e.g. Merow et al. 2011). This drawback also affects other  
362 types of biodiversity models such as stacked species distribution models (Pottier et al. 2013)  
363 leading to inaccurate predictions of community structure at small spatial scales (Thuiller et al.  
364 2015). This has long been interpreted as a consequence of not properly accounting for biotic  
365 interactions. Our study supports for this conjecture: including competitive interactions improves  
366 the modeling of species occurrences and further decreases the predicted diversity ( $\alpha$ -diversity)  
367 and increases the predicted turnover ( $\beta$ -diversity) bringing them closer to the observed diversity  
368 values (Supplementary Figure 4). Our results follow the classical expectation that the realized  
369 niche of species is smaller than the fundamental niche because species interactions limit where  
370 species actually occur (MacArthur & Levins 1967). In more details, the assembly model that  
371 include only abiotic filtering predicts remarkably even species abundances (Figure 3,  
372 Supplementary figure 5), in contrast with the usual strong heterogeneity that characterizes  
373 species abundance distributions (McGill et al. 2007). The inclusion of biotic interactions  
374 predicts a more realistic distribution of species abundances within communities and produces  
375 more sparse species-by-site community matrices that exhibited a stronger hierarchy among  
376 species (Figure 3, Supplementary figure 5).

377 By applying our framework to the strong flooding gradient in a wetland ecosystem, we were  
378 able to get insights into the ecological mechanisms that determine wetland community structure  
379 and also identify our framework limitations. First, we found that a trait-based model of abiotic  
380 filtering (root porosity, SLA, and height) led to a modest improvement in model fit compared to  
381 the null model (Table 1, pseudo  $R^2$  95% IQ [0.075, 0.085]). This suggested flooding filtered the  
382 species pool primarily by porous root tissue that enhances the ability of species to tolerate  
383 flooded and anoxic soil (Moor et al. 2017; Tanentzap & Lee 2017). When we added trait-based  
384 competitive interactions to this assembly model, we significantly improved the modeling of  
385 species covers and, consequently, of community structure. Using traits to estimate the  
386 interaction matrix further proved useful as the assembly model with a fixed pairwise interaction  
387 matrix was not well supported by the data. The “best” model was the model that calibrated  
388 biotic interactions with SLA (Table 1, pseudo  $R^2$  95% IQ [0.182, 0.196]). This suggests that

389 competitive interactions among plants in that ecosystem could be mediated through leaf  
390 economics (Violle et al. 2009; Tanentzap & Lee 2017). In contrast, the interaction matrix  
391 calibrated only with height was less supported by the data. This indicated that there was little  
392 competitive interference among pairs with dissimilar SLA values, likely because they partition  
393 resources and are thus able to coexist (Moor et al. 2017).

394 However, even the best assembly model explained a relatively modest portion of species  
395 abundances. This points both to the limitations of the available data and of our framework. Only  
396 root porosity was found to vary, and only moderately, along the flooding gradient (adjusted  $R^2 =$   
397 0.21). Thus the modeled carrying capacities of species along the flooding did not vary as  
398 strongly as could be *a priori* expected (see Figure 3). The intraspecific variability of root  
399 porosity was important (32% of total root porosity variance was intraspecific) and may dampen  
400 our ability to use this trait to model species' abiotic niche (Read et al. 2017). It is also possible  
401 that other unmeasured functional traits may be involved in the filtering of species along the  
402 flooding gradient (Moor et al. 2017).

## 403 **Conclusion**

404 It has been argued that complex ecological processes can be modeled with limited data input by  
405 leveraging the generality of functional traits (McGill et al. 2006). In community ecology,  
406 functional traits are mainly used in diversity pattern analyses codified by assembly theory  
407 (Keddy 1992). Those analyses have numerous pitfalls: non-random functional diversity patterns  
408 can be interpreted in multiple ways thus rendering difficult a confident inference of community  
409 assembly rules (Kraft et al. 2015b; Cadotte & Tucker 2017; Münkemüller et al. 2020). In  
410 contrast, our approach specifies explicit assembly rules and model directly local species  
411 abundances. Ultimately, our framework provides a process-based approach to predict  
412 community structure and quantify its support. Such trait-based modelling opens a new general  
413 way to model natural communities and will improve our ability to understand and predict  
414 biodiversity structure and dynamics under global change.

415

## 416 **Acknowledgments**

417 This research was supported by funding from both the University of Waikato and Manaaki  
418 Whenua - Landcare Research. John Payne of Landcare Research kindly provided the  
419 capacitance probe water level data. We call our new model, 'Banquo', in honor of Bill Shipley,

420 who, in his foundational book (Shipleigh 2010) was the first to highlight Banquo’s desire to  
421 predict ‘which grain will grow and which will not’ in Shakespeare’s Macbeth. LC acknowledges  
422 a postdoctoral fellowship at the University of Wyoming and funding from the European Union’s  
423 Horizon 2020 research and innovation program under the Marie Skłodowska-Curie grant  
424 agreement No 840946 (Project “CLIMB”). DBS acknowledges the support of a Rutherford  
425 Discovery Fellowship and the Marsden Fund Council from New Zealand Government funding,  
426 both of which are managed by the Royal Society of New Zealand Te Apārangi (RDF-13-UOC-  
427 003 and 16-UOC-008), and an Erskine Grant from the University of Canterbury.

428 **Author Contributions**

429 LC, DBS and DCL led the study. LC developed and ran the analyses and wrote the first draft.  
430 ASTP, WGL, AJT and DCL collected the data. All authors contributed to the writing of the  
431 paper.

432

433 **Table 1. Comparison of the assembly models.** Each model posterior is described by the  
 434 Deviance Information criterion (DIC), Nagelkerke's pseudo  $R^2$ , the area under the curve (AUC)  
 435 and Gelman's multivariate convergence criterion (MPSRF). The assembly models are ranked by  
 436 decreasing median pseudo  $R^2$ .

Assembly model category	Traits used to calibrate interactions ( $\alpha_{ik}$ )	Fixed parameters	Parameters to estimate	MPSRF	DIC	Pseudo $R^2$	AUC
Abiotic & Biotic model	SLA	/	$a, b, C, \mu, \sigma, \varphi$	1.002	2291	[0.182, 0.196]	0,773
Abiotic & Biotic model	Height + SLA (with int.)	/	$a, b, C, \mu_1, \mu_2, \sigma_1, \sigma_2, \rho, \varphi$	1.004	2295	[0.177, 0.194]	0,773
Abiotic & Biotic model	Height + SLA (no int.)	/	$a, b, C, \mu_1, \mu_2, \sigma_1, \sigma_2, \varphi$	1.018	2308,8	[0.171, 0.188]	0,764
Abiotic & Biotic model	Height	/	$a, b, C, \mu, \sigma, \varphi$	1.000	2371,8	[0.115, 0.13]	0,689
Abiotic model	No interactions	$\alpha = I$	$a, b, \varphi$	1.000	2413,8	[0.075, 0.085]	0,671
Abiotic & Biotic model	No traits	$\sigma \rightarrow \infty$	$a, b, C', \varphi$	1.001	2412	[0.071, 0.082]	0,669
Biotic model	Height + SLA (with int.)	$b = 0$	$a, C, \mu_1, \mu_2, \sigma_1, \sigma_2, \rho, \varphi$	1.811	/	[0.056, 0.088]	/
Biotic model	Height + SLA (no int.)	$b = 0$	$a, C, \mu_1, \mu_2, \sigma_1, \sigma_2, \varphi$	1.021	2415,2	[0.038, 0.067]	0,657
Biotic model	SLA	$b = 0$	$a, C, \mu, \sigma, \varphi$	1.006	2420,7	[0.03, 0.043]	0,631
Biotic model	Height	$b = 0$	$a, C, \mu, \sigma, \varphi$	1.025	2456	[0.027, 0.042]	0,574
Biotic model	No traits	$b = 0, \sigma \rightarrow \infty$	$a, C', \varphi$	1.000	2491,8	[0, 0.001]	0,448
Null model	No interactions	$\alpha = I, b = 0$	$a, \varphi$	1.000	2491,8	[0, 0.001]	0,5



437 **Figure 1. Relationship between the duration of flooding and plant traits:** root porosity (a),  
438 specific leaf area (b) and vegetative height (c). Data point size is proportional to plant cover. The  
439 line indicates the modeled relationship used in the Traitspace framework. The three linear  
440 models were all statistically significant (Root porosity, adjusted  $R^2 = 0.206$ ,  $p < 1 \times 10^{-5}$  ;  
441 Specific leaf area, adjusted  $R^2 = 0.037$ ,  $p = 0.0021$ ; Vegetative height, adjusted  $R^2 = 0.060$ ,  $p$   
442  $=0.0001$ ).

443 **Figure 2. Calibrated pairwise interaction coefficients of the abiotic and biotic assembly**  
444 **models.** The graphic represents interspecific  $\alpha_{ij}$  (competitive impact of species  $j$  on species  $i$ ) as  
445 a function of the height-only (a), SLA-only (b), or both (c,d) differences of species  $i$  and species  
446  $j$ . The blue scale represents the absolute value of the pairwise coefficient. To facilitate the  
447 interpretation of the two-traits plots (c-d), we indicated the position of the largest pairwise  
448 interaction coefficient value with an orange diamond.

449 **Figure 3. Comparison of observed and modeled species cover along the flooding gradient.**  
450 Red response curves are fitted on the species cover as predicted by the abiotic model. Green  
451 response curves are fitted on the species cover as predicted by the best abiotic and biotic model  
452 (see Table 1). Black nonlinear response curves are fitted directly to the observed cover for each  
453 species. All curves are fitted using a loess function.

454

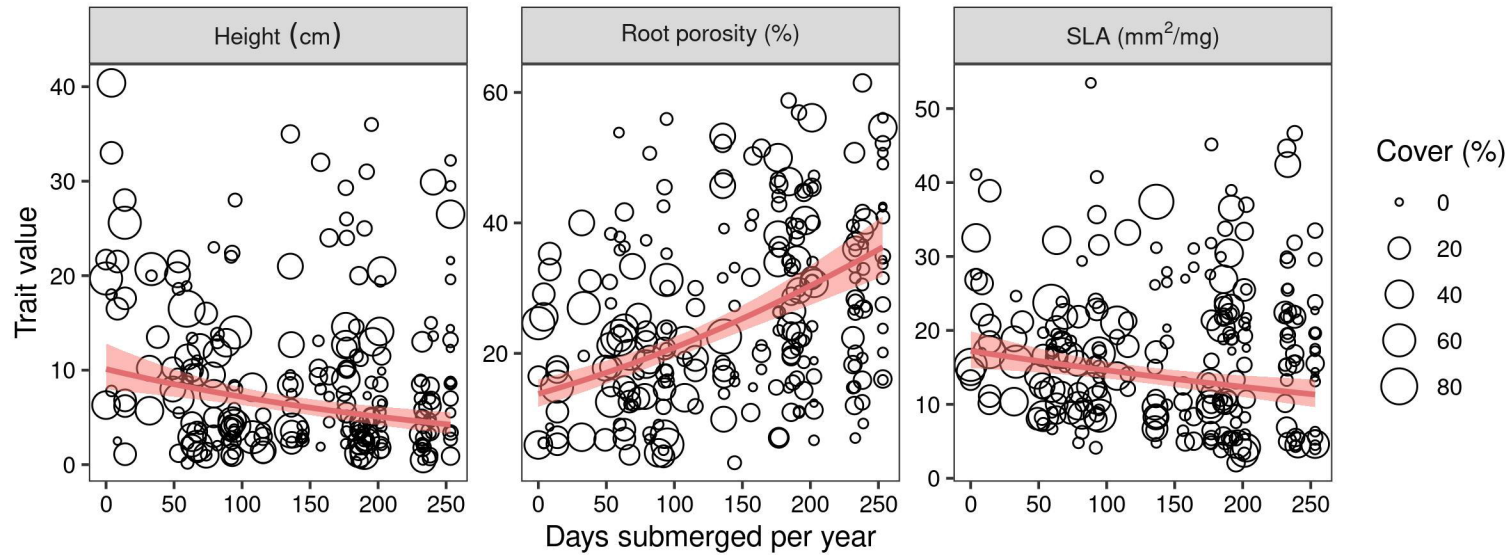
## 455 **References**

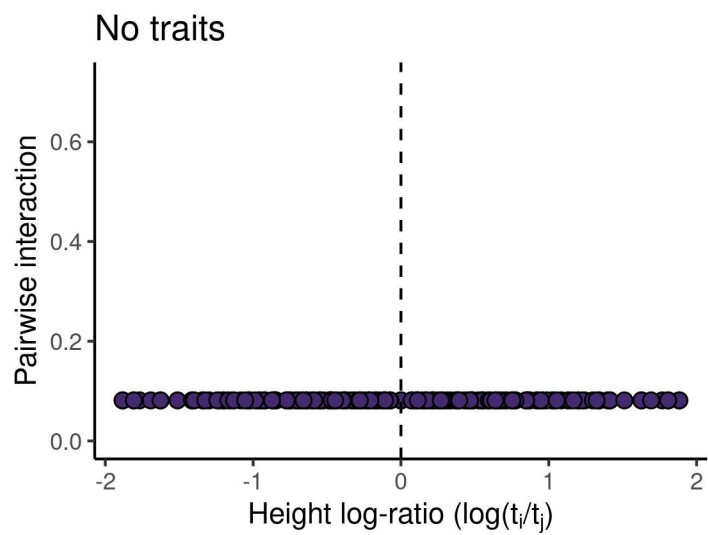
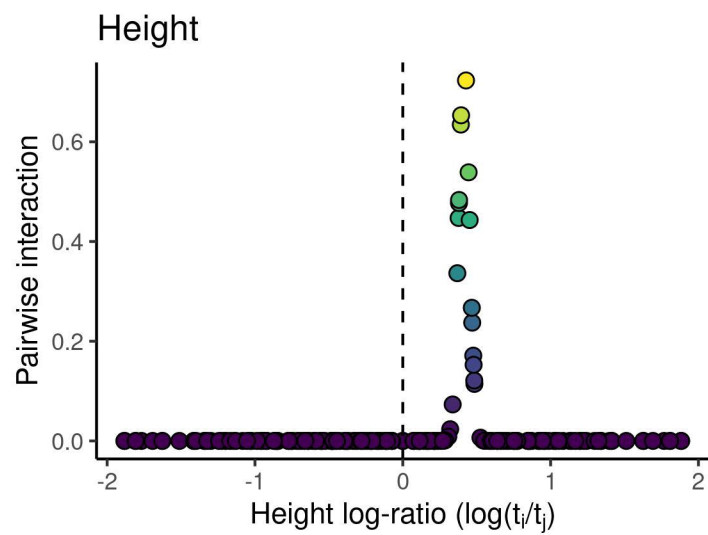
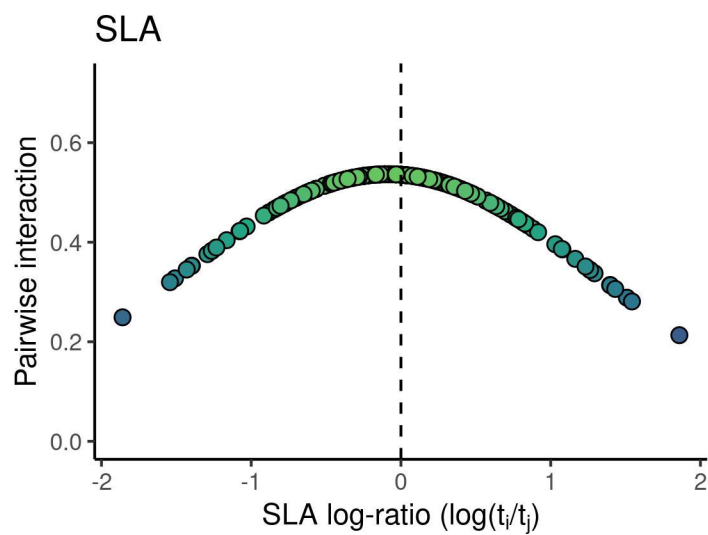
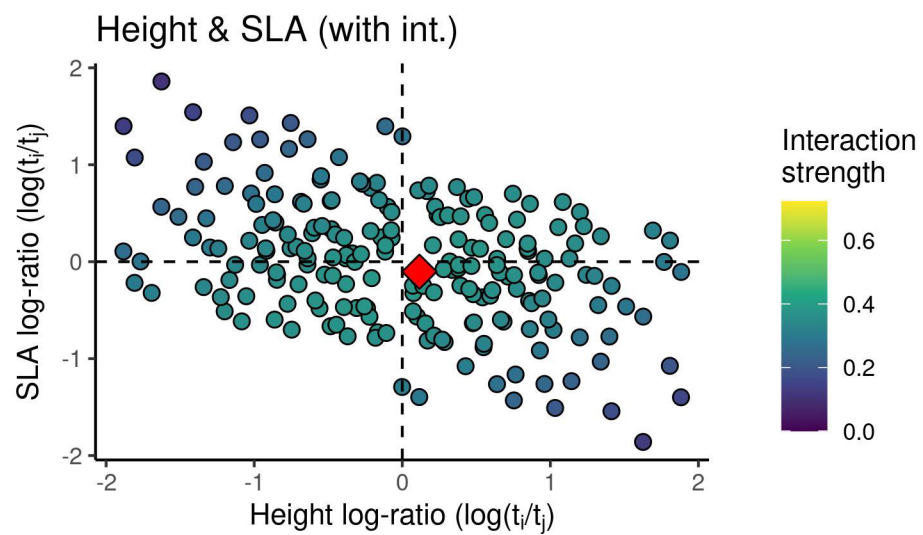
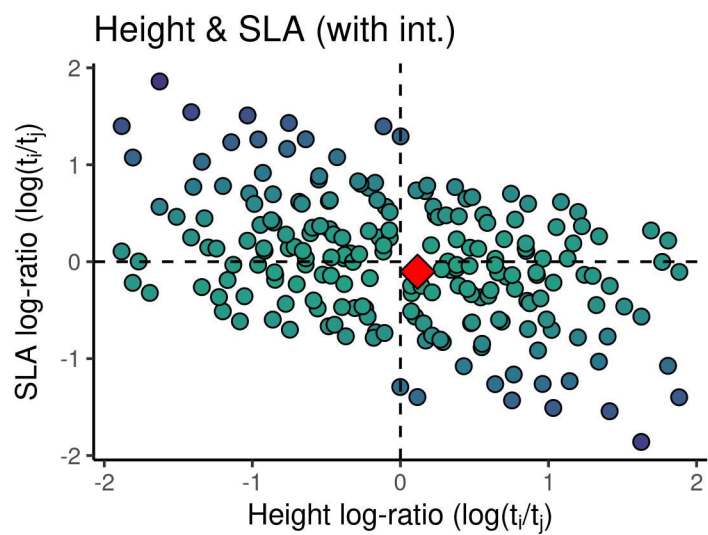
- Adler, P.B., HilleRisLambers, J. & Levine, J.M. (2007). A niche for neutrality. *Ecology Letters*, 10, 95–104.
- Alexander, J.M., Diez, J.M. & Levine, J.M. (2015). Novel competitors shape species' responses to climate change. *Nature*, 525, 515–518.
- Banner, K.M., Irvine, K.M. & Rodhouse, T. (2020). The Use of Bayesian Priors in Ecology: The Good, The Bad, and The Not Great. *Methods in Ecology and Evolution*, 00, 1–8.
- Bimler, M.D., Stouffer, D.B., Lai, H.R. & Mayfield, M.M. (2018). Accurate predictions of coexistence in natural systems require the inclusion of facilitative interactions and environmental dependency. *Journal of Ecology*, 106, 1839–1852.
- Cabral, J.S., Valente, L. & Hartig, F. (2017). Mechanistic simulation models in macroecology and biogeography: state-of-art and prospects. *Ecography*, 40, 267–280.
- Cadotte, M.W. & Tucker, C.M. (2017). Should Environmental Filtering be Abandoned? *Trends in Ecology & Evolution*, 32, 429–437.
- Chalmandrier, L., Hartig, F., Laughlin, D.C., Lischke, H., Pichler, M., Stouffer, D.B., *et al.* (2021). Linking functional traits and demography to model species-rich communities. *Nature Communications*.
- Chalmandrier, L., Münkemüller, T., Colace, M.-P., Renaud, J., Aubert, S., Carlson, B.Z., *et al.* (2017). Spatial scale and intraspecific trait variability mediate assembly rules in alpine grasslands. *J Ecol*, 105, 277–287.
- Chesson, P. (2000). Mechanisms of maintenance of species diversity. *Annual review of Ecology and Systematics*, 343–366.
- Damgaard, C.F. & Irvine, K.M. (2019). Using the beta distribution to analyse plant cover data. *Journal of Ecology*, 107, 2747–2759.
- Evans, M.E., Merow, C., Record, S., McMahon, S.M. & Enquist, B.J. (2016). Towards process-based range modeling of many species. *Trends in Ecology & Evolution*, 31, 860–871.

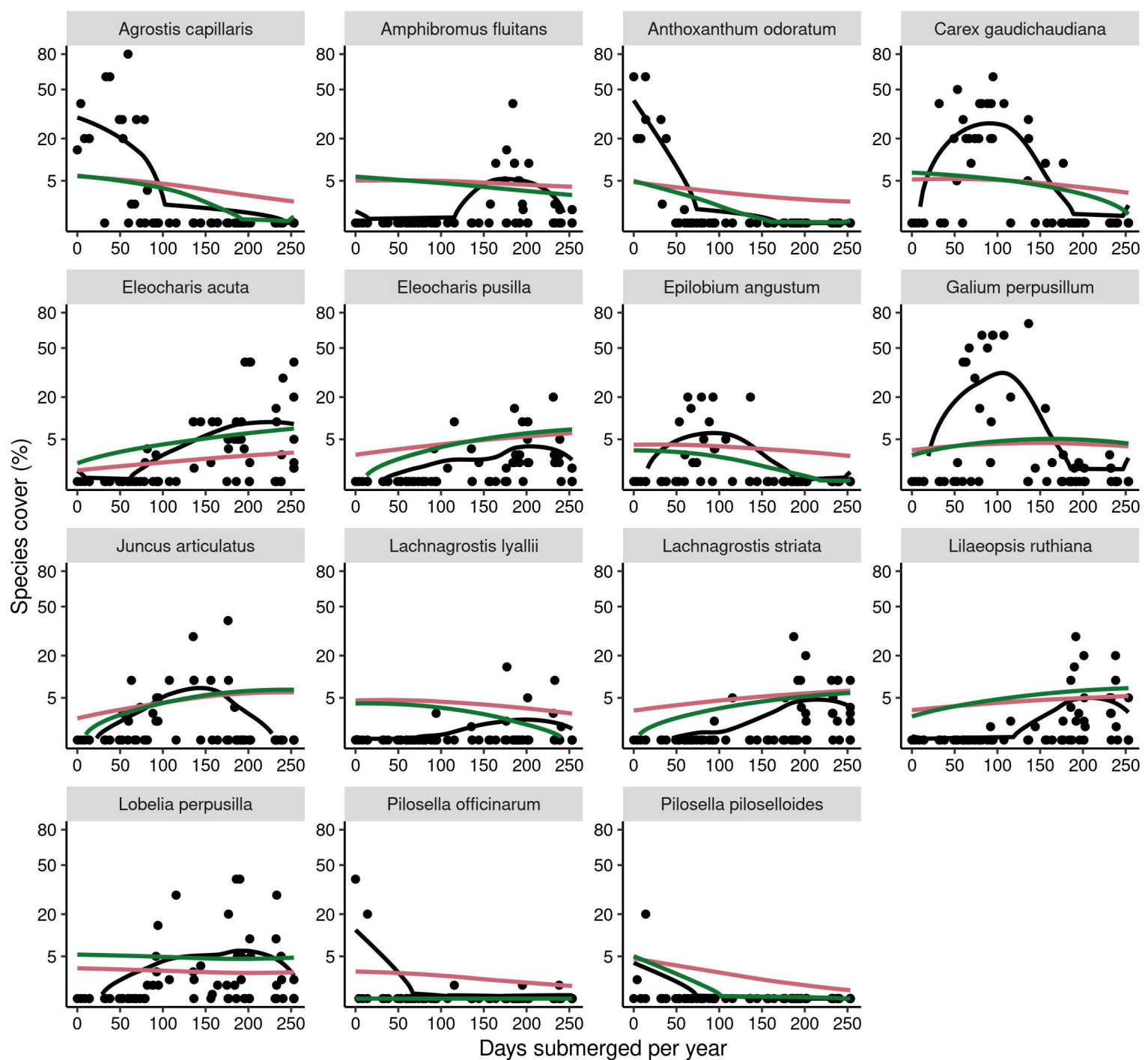
- Falster, D.S., Brännström, A., Westoby, M. & Dieckmann, U. (2017). Multitrait successional forest dynamics enable diverse competitive coexistence. *Proceedings of the National Academy of Sciences*, 114, E2719–E2728.
- Gelman, A., Hwang, J. & Vehtari, A. (2014). Understanding predictive information criteria for Bayesian models. *Statistics and computing*, 24, 997–1016.
- Hartig, F., Minunno, F. & Paul, S. (2017). BayesianTools: General-Purpose MCMC and SMC Samplers and Tools for Bayesian Statistics. *R package*.
- HilleRisLambers, J., Adler, P.B., Harpole, W.S., Levine, J.M. & Mayfield, M.M. (2012). Rethinking community assembly through the lens of coexistence theory. *Annual Review of Ecology, Evolution, and Systematics*, 43, 227.
- Irvine, K.M., Wright, W.J., Shanahan, E.K. & Rodhouse, T.J. (2019). Cohesive framework for modelling plant cover class data. *Methods in Ecology and Evolution*, 10, 1749–1760.
- Keddy, P.A. (1992). Assembly and response rules: two goals for predictive community ecology. *Journal of Vegetation Science*, 3, 157–164.
- Keddy, P.A. (2001). *Competition*. Springer.
- Kraft, N.J., Godoy, O. & Levine, J.M. (2015a). Plant functional traits and the multidimensional nature of species coexistence. *Proceedings of the National Academy of Sciences*, 112, 797–802.
- Kraft, N.J.B., Adler, P.B., Godoy, O., James, E.C., Fuller, S. & Levine, J.M. (2015b). Community assembly, coexistence and the environmental filtering metaphor. *Funct Ecol*, 29, 592–599.
- Laughlin, D.C., Joshi, C., van Bodegom, P.M., Bastow, Z.A. & Fulé, P.Z. (2012). A predictive model of community assembly that incorporates intraspecific trait variation. *Ecol Lett*, 15, 1291–1299.
- Letten, A.D., Ke, P.-J. & Fukami, T. (2017). Linking modern coexistence theory and contemporary niche theory. *Ecological Monographs*, 87, 161–177.
- Lotka-Volterra, A.J. (1925). *Elements of physical biology*. Williams & Wilkins Co, Baltimore.
- MacArthur, R. & Levins, R. (1967). The limiting similarity, convergence, and divergence of coexisting species. *American naturalist*, 377–385.
- Maestre, F.T., Callaway, R.M., Valladares, F. & Lortie, C.J. (2009). Refining the stress-gradient hypothesis for competition and facilitation in plant communities. *Journal of Ecology*, 97, 199–205.

- McGill, B.J., Enquist, B.J., Weiher, E. & Westoby, M. (2006). Rebuilding community ecology from functional traits. *Trends in ecology & evolution*, 21, 178–185.
- McGill, B.J., Etienne, R.S., Gray, J.S., Alonso, D., Anderson, M.J., Benecha, H.K., *et al.* (2007). Species abundance distributions: moving beyond single prediction theories to integration within an ecological framework. *Ecology Letters*, 10, 995–1015.
- Merow, C., Latimer, A.M. & Silander, J.A. (2011). Can entropy maximization use functional traits to explain species abundances? A comprehensive evaluation. *Ecology*, 92, 1523–1537.
- Moor, H., Rydin, H., Hylander, K., Nilsson, M.B., Lindborg, R. & Norberg, J. (2017). Towards a trait-based ecology of wetland vegetation. *Journal of Ecology*, 105, 1623–1635.
- Münkemüller, T., Gallien, L., Barros, C., Carboni, M., Chalmandrier, L., Mazel, F., *et al.* (2020). Do's and don'ts when inferring assembly rules from diversity patterns, 29, 1212–1229.
- Nagelkerke, N.J. (1991). A note on a general definition of the coefficient of determination. *Biometrika*, 78, 691–692.
- Nakagawa, S. & Schielzeth, H. (2013). A general and simple method for obtaining R<sup>2</sup> from generalized linear mixed-effects models. *Methods Ecol Evol*, 4, 133–142.
- Pakeman, R.J. & Quested, H.M. (2007). Sampling plant functional traits: What proportion of the species need to be measured? *Applied Vegetation Science*, 10, 91–96.
- Pottier, J., Dubuis, A., Pellissier, L., Maiorano, L., Rossier, L., Randin, C.F., *et al.* (2013). The accuracy of plant assemblage prediction from species distribution models varies along environmental gradients. *Global Ecology and Biogeography*, 22, 52–63.
- Purcell, A.S.T., Lee, W.G., Tanentzap, A.J. & Laughlin, D.C. (2019). Fine Root Traits Are Correlated with Flooding Duration while Aboveground Traits Are Related to Grazing in an Ephemeral Wetland. *Wetlands*, 39, 291–302.
- Read, Q.D., Henning, J.A. & Sanders, N.J. (2017). Intraspecific variation in traits reduces ability of trait-based models to predict community structure. *Journal of Vegetation Science*, 28, 1070–1081.
- Robin, X., Turck, N., Hainard, A., Tiberti, N., Lisacek, F., Sanchez, J.-C., *et al.* (2011). pROC: an open-source package for R and S+ to analyze and compare ROC curves. *BMC Bioinformatics*, 12, 77.

- Scrucca, L., Fop, M., Murphy, T.B. & Raftery, A.E. (2016). mclust 5: clustering, classification and density estimation using Gaussian finite mixture models. *The R journal*, 8, 289.
- Shipley, B. (2010). *From plant traits to vegetation structure: chance and selection in the assembly of ecological communities*. Cambridge University Press.
- Spasojevic, M.J., Copeland, S. & Suding, K.N. (2014). Using functional diversity patterns to explore metacommunity dynamics: a framework for understanding local and regional influences on community structure. *Ecography*, 37, 939–949.
- Tanentzap, A.J. & Lee, W.G. (2017). Evolutionary conservatism explains increasing relatedness of plant communities along a flooding gradient. *New Phytologist*, 213, 634–644.
- Tanentzap, A.J., Lee, W.G., Monks, A., Ladley, K., Johnson, P.N., Rogers, G.M., *et al.* (2014). Identifying pathways for managing multiple disturbances to limit plant invasions. *Journal of Applied Ecology*, 51, 1015–1023.
- Thuiller, W., Pollock, L.J., Gueguen, M. & Münkemüller, T. (2015). From species distributions to meta-communities. *Ecology letters*, 18, 1321–1328.
- Violle, C., Garnier, E., Lecoqeur, J., Roumet, C., Podgeur, C., Blanchard, A., *et al.* (2009). Competition, traits and resource depletion in plant communities. *Oecologia*, 160, 747–755.
- Violle, C., Navas, M.L., Vile, D., Kazakou, E., Fortunel, C., Hummel, I., *et al.* (2007). Let the concept of trait be functional! *Oikos*, 116, 882–892.
- Zakharova, L., Meyer, K.M. & Seifan, M. (2019). Trait-based modelling in ecology: A review of two decades of research. *Ecological Modelling*, 407, 108703.



**A****B****C****D****E**



— Observed — Abiotic model — Abiotic + Biotic model